Supporting information for:

Inhibition of the Side Reactions and Dendrite Growth by the Low-cost and Non-flammable Eutectic Electrolyte for High-voltage and Super-stable Zinc Hybrid Battery

Yongqi Deng, Yihan Wu, Kefu Zhang, Minghui Fan, Lele Wang, Yapeng He, Lifeng Yan*

Department of Chemical Physics, University of Science and Technology of China, Jinzai road 96, Hefei, 230026, Anhui, China.

Corresponding author: Lifeng Yan, Fax/Tel: +86-551-63606853;

E-mail: lfyan@ustc.edu.cn

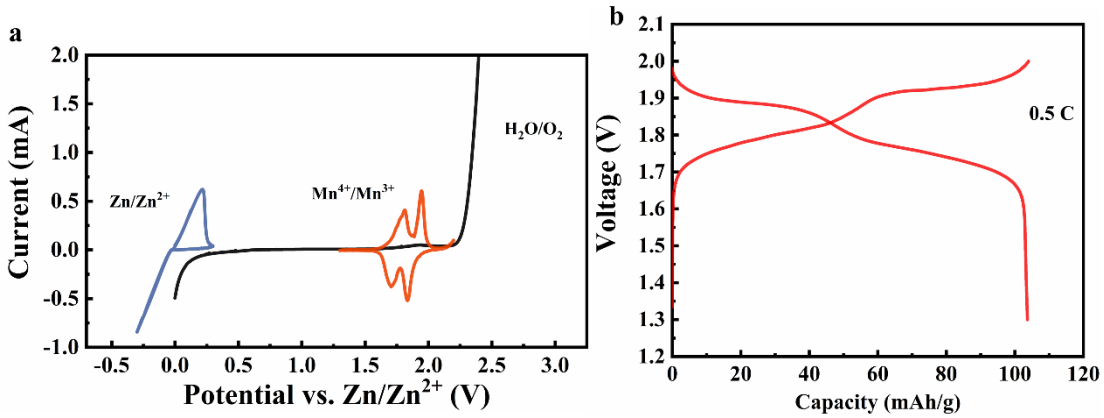

Figure S1. (a) The ESW of AQ electrolyte at a scan rate of 5 mV s^{-1} on stainless steel electrodes (blank line) and redox potential of LMO positive electrode and Zn negative electrode vs. Zn/Zn^{2+}. (b) Typical voltage profile of the Zn//LMO full battery using AQ electrolyte at constant current (0.5 C).

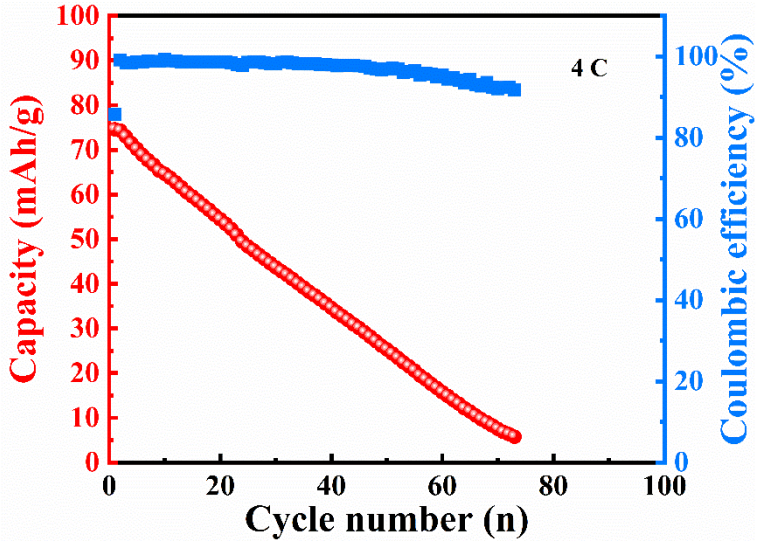

Figure S2. Cycling stability and coulombic efficiency of Zn//LMO full battery using AQ electrolyte (at 4 C).

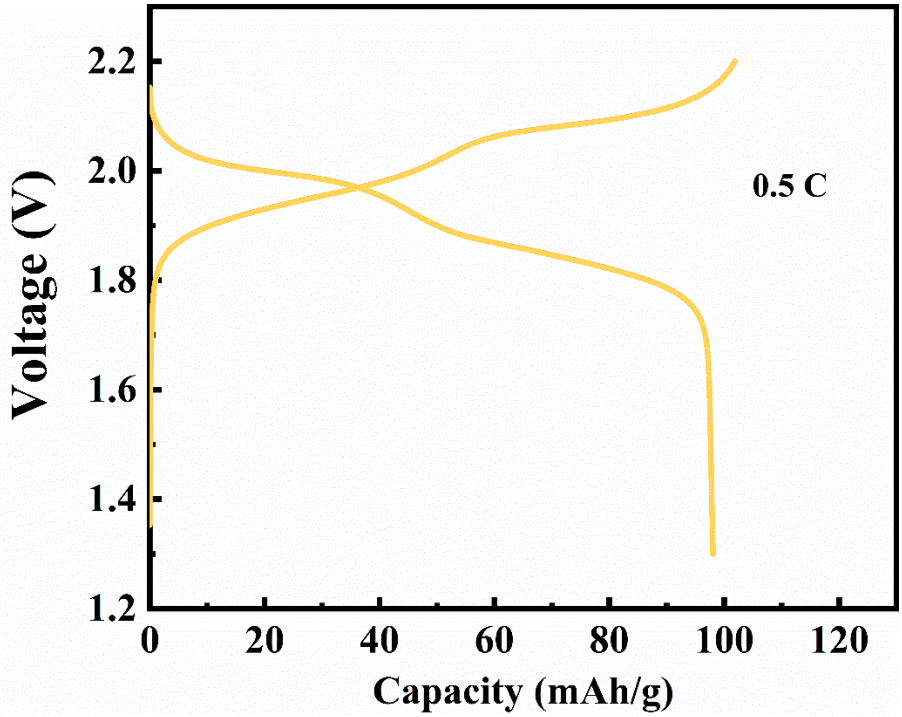

Figure S3. Typical voltage profile of the Zn//LMO full battery using ZLU eutectic electrolyte at constant current (0.5 C).

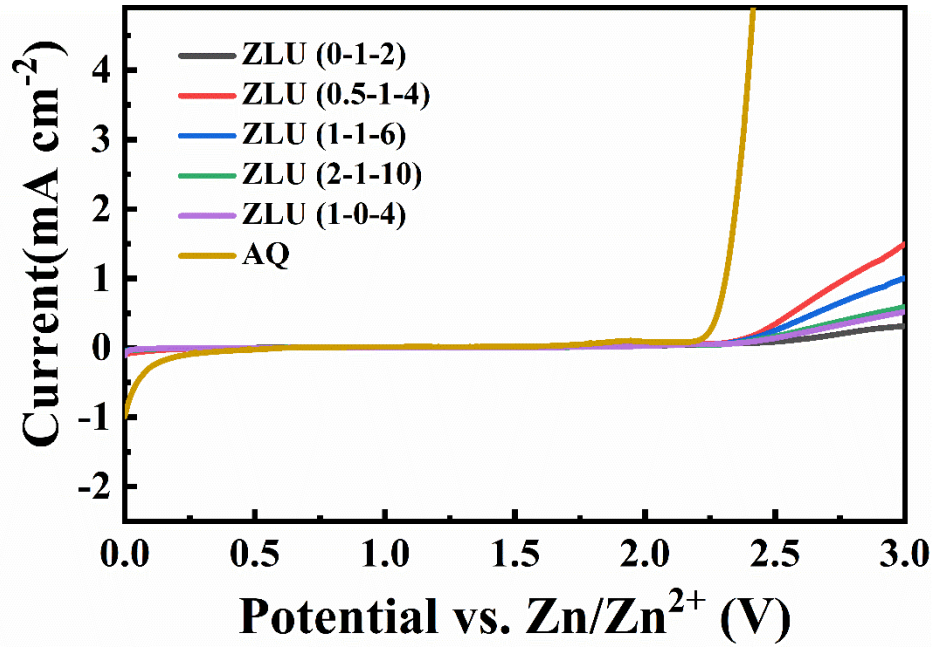

Figure S4. ESWs of eutectic electrolytes with different molar ratios at a scan rate of 5 mV s^{-1}.

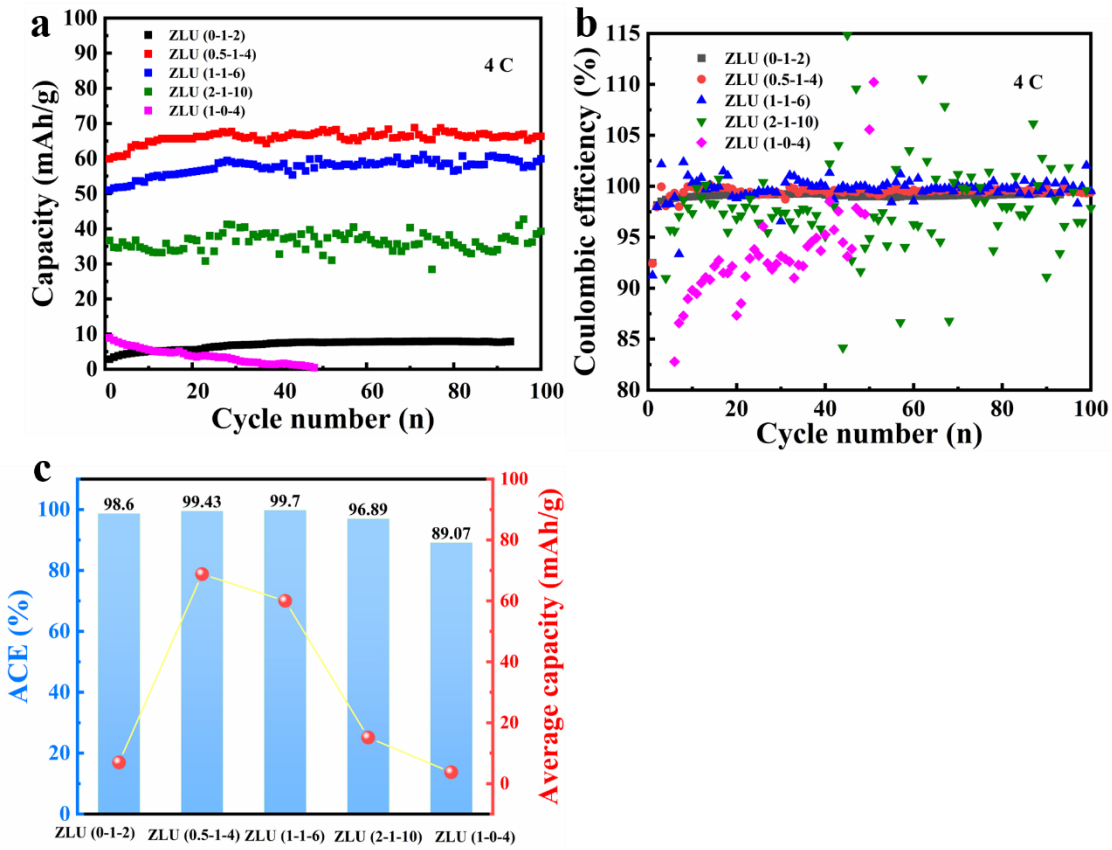

Figure S5. Cycling stability (a) and coulombic efficiency (b) of Zn//LMO full battery using eutectic electrolyte with different molar ratios (at 4 C). (c) Average capacity and coulombic efficiency of Zn//LMO full battery using eutectic electrolyte with different molar ratios (at 4 C).

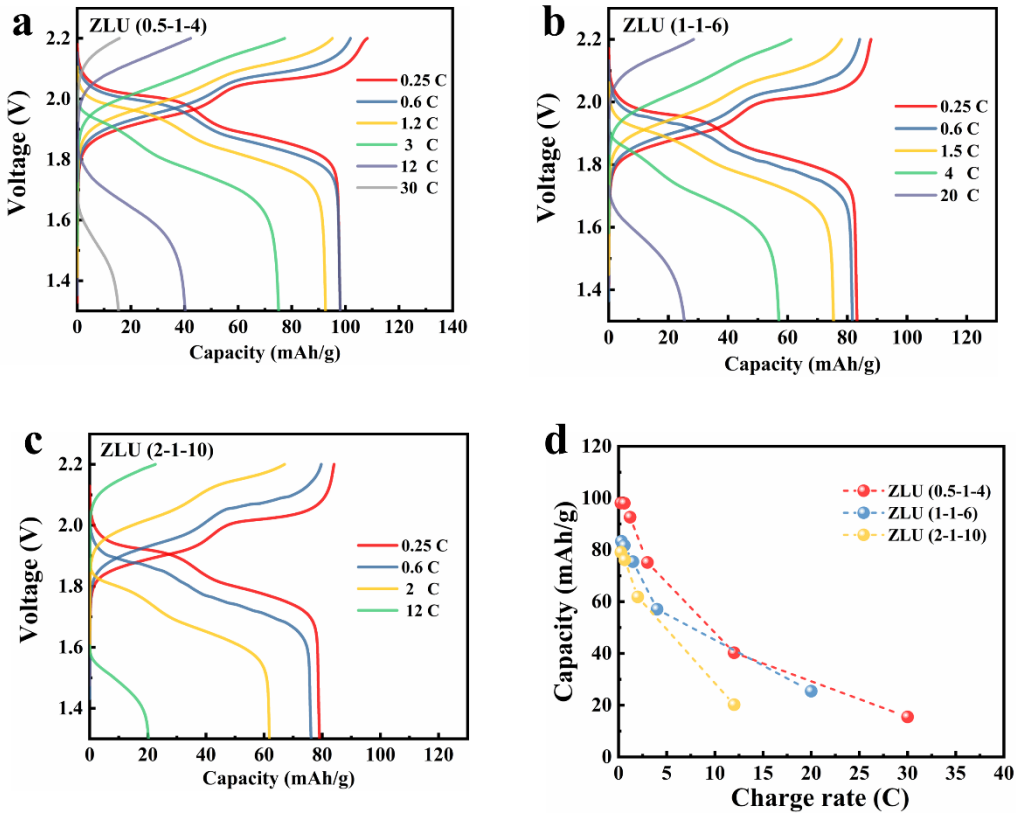

Figure S6. The rate capability (Zn//LMO) in ZLU eutectic electrolyte: (a) ZLU (0.5-1-4) at 0.25 C, 0.6 C, 1.2 C, 3 C, 12 C and 30 C; (b) ZLU (1-1-6) at 0.25 C, 0.6 C, 1.5 C, 4 C, 20 C; (c) ZLU (2-1-10) at 0.25 C, 0.6 C, 2 C, 3 C, 12 C. (d) Comparison of rate capability (Zn//LMO) using ZLU eutectic electrolyte with different molar ratios.

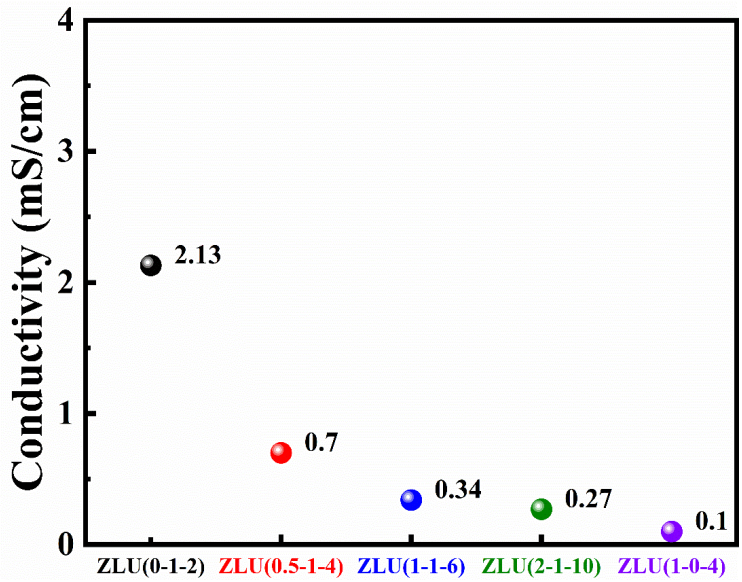

Figure S7. Ionic conductivity of ZLU eutectic electrolyte with different molar ratios at 25 °C.

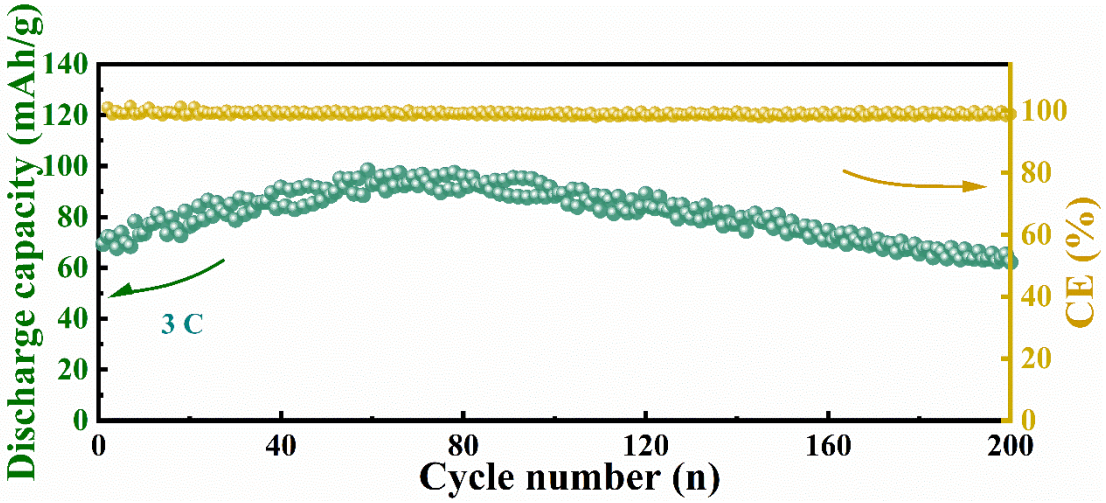

Figure S8. Cycling stability and coulombic efficiency of Zn//LMO full battery employing ZLU (0.5-1-4) eutectic electrolyte at 3 C.

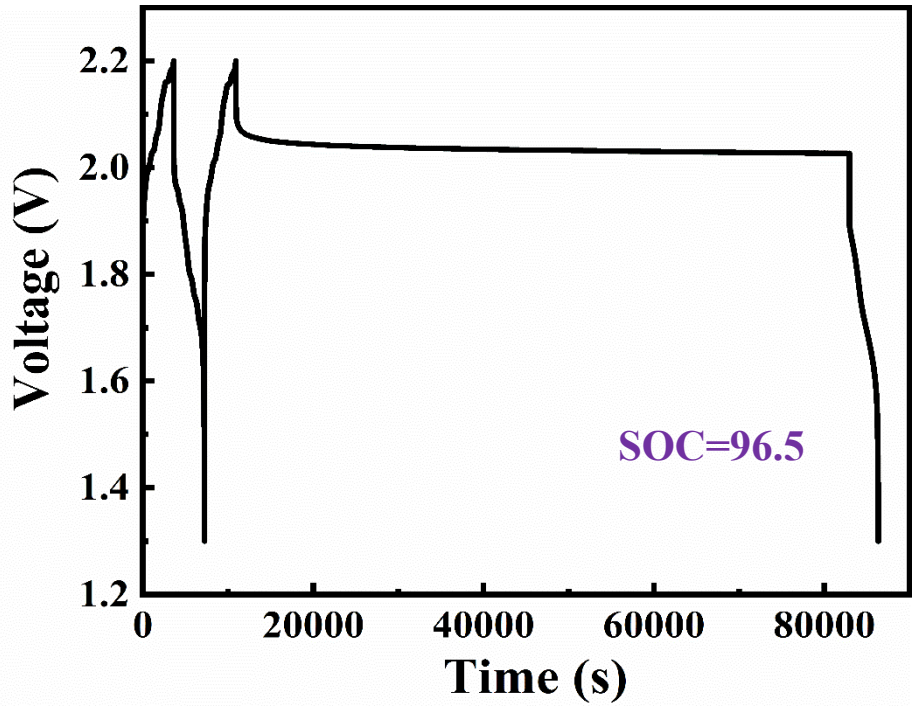

Figure S9. Storage performance of Zn//LMO full battery employing ZLU eutectic electrolyte evaluated by resting for 24 h at 100% state of charge (SOC) after five cycles at 0.5 C, followed by full discharging.

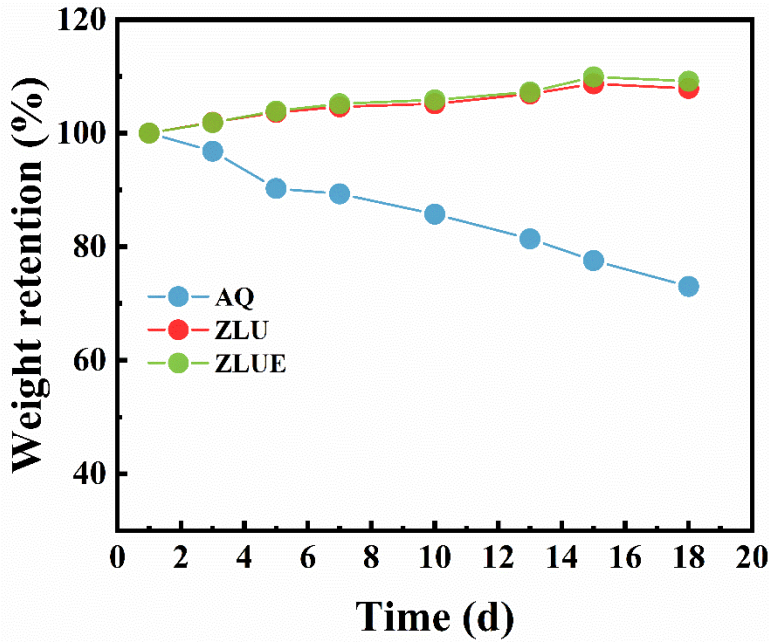

Figure S10. Volatility tests of AQ electrolyte and ZLU eutectic electrolyte in the atmosphere for 18 days at room temperature.

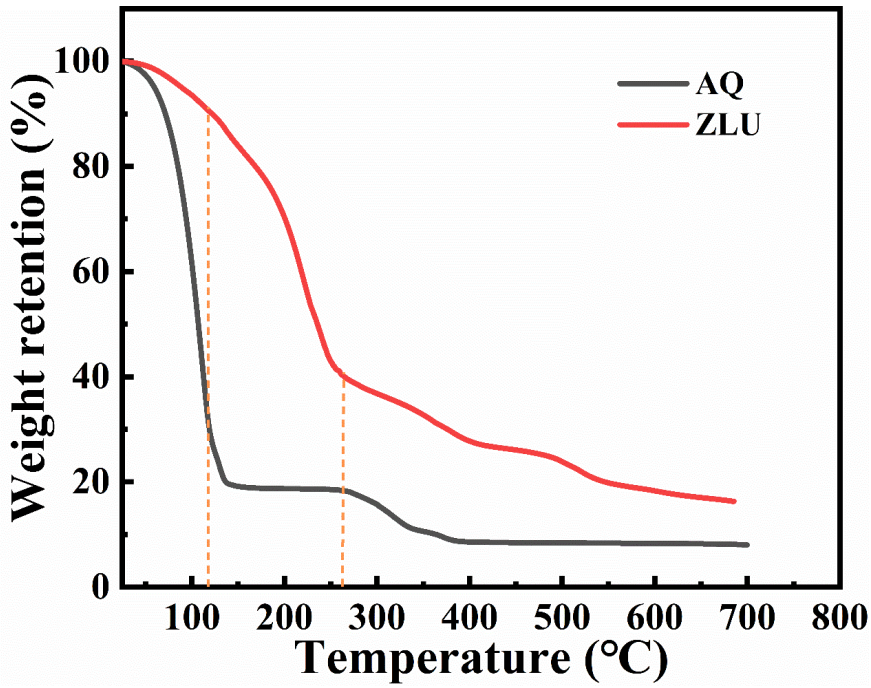

Figure S11. Thermogravimetric analysis of AQ electrolyte and ZLU eutectic electrolyte in the N_2 atmosphere with 10 °C/min.

Table S1. Comparison of composition, price and ionic conductivity between our developed eutectic electrolyte and reported representative TFSI-based high-

concentration electrolyte. (Price data were collected from Shanghai Aladdin Biochemical Technology Co.).

Electrolyte	**Composition(wt%)**	**Price (US$/kg)**	**Ionic conductivity (mS cm^{-1})**	**Ref.**
"Water-in-Salt" 21m LiTFSI	LiTFSI: 85.8 H_2O: 14.2	314	8.21 (25℃)	1
"Water-in-Bisalt" 21 m LiTFSI-7 m LiOTf	LiTFSI: 74.2 LiOTf: 13.5 H_2O: 12.3	347.6	6.5 (25℃)	2
Hydrate Melt" $Li(TFSI)_{0.7}(BETI)_{0.3}·2H_2O$ 19.4 m LiTFSI-8.3 m LiBETI)	LiTFSI:56.9 LiBETI:32.9 H_2O:10.2	14552	3.0 (30℃)	3
"Hybrid Aqueous/Nonaqueous" 21 m LiTFSI in H_2O-9.25 m LiTFSI in DMC (wt%=1:1)	LiTFSI: 81.2 DMC: 9.4 H_2O: 9.4	297.3	5.0 (30℃)	4
"Monohydrate Melt" $Li(PTFSI)_{0.6}(TFSI)_{0.4}·1H_2O$ 22.2m LiTFSI-33.3 m LiPTFSI)	LiTFSI: 34.2 LiPTFSI: 60.4 H_2O: 5.4	N/A	0.1 (30℃)	5
$Li(TFSI)_{0.8}(MM3411)_{0.2}·1.4$ H_2O 31.4m LiTFSI-7.9 m LiMM3411	LiTFSI:72.4 LiMM3411:19.6 H_2O:8.0	N/A	0.33 (25℃)	6
$ZnAc_2$+LiAc+urea	$ZnAc_2$:20.3 LiAc:14.6 Urea:53.1 H_2O:12	23.7	0.7 (25℃)	This work
$ZnAc_2$+LiAc+urea+EG	$ZnAc_2$:17.8 LiAc:12.7 Urea:46.3 EG:12.7 H_2O:10.5	22.1	2.34 (25℃)	This work

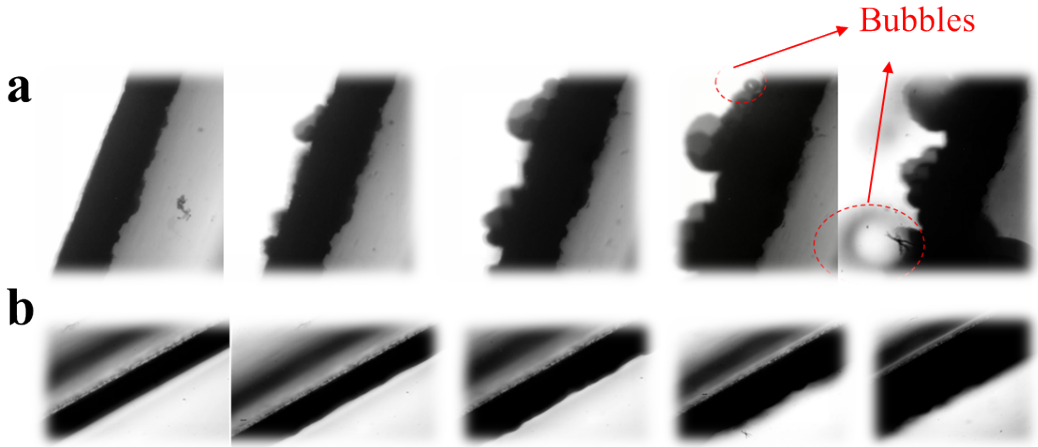

Figure S12. In situ observation of Zn plating in AQ (a) and ZLU (b) electrolyte by optical microscopy at a current density of 1 mA cm-2 for 5h.

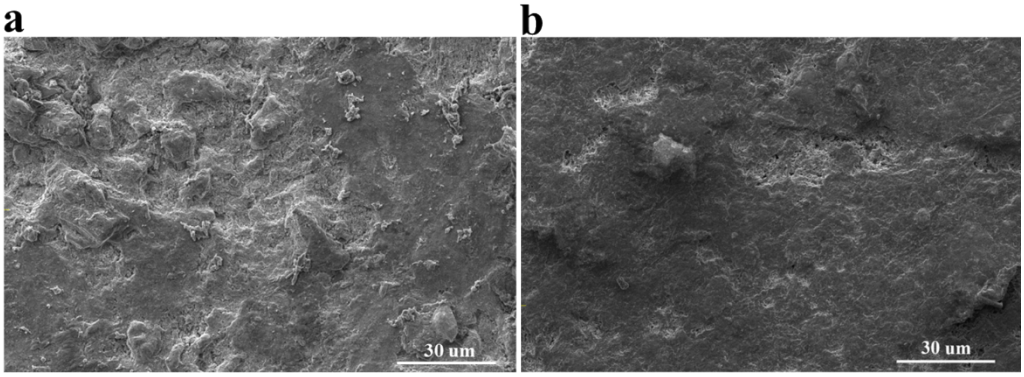

Figure S13. SEM images of the Zn anode after plating in the reference AQ electrolyte (a) and ZLU eutectic electrolyte (b).

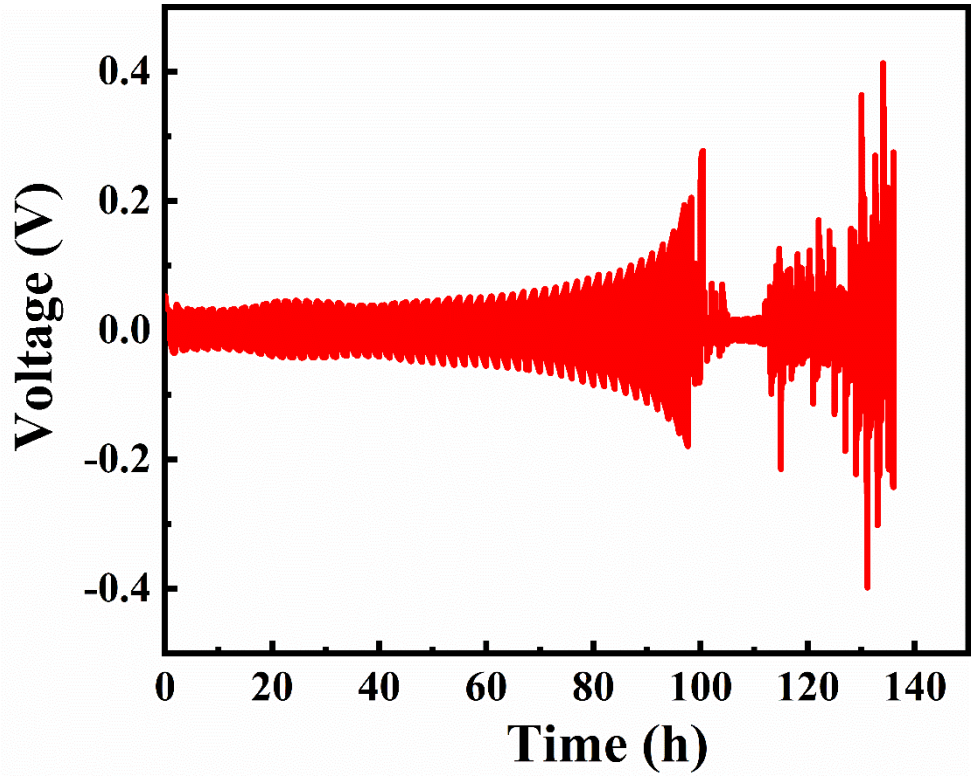

Figure S14. Galvanostatic Zn plating/stripping in Zn//Zn symmetrical cells with AQ electrolyte at 0.5 mA cm^{-2} and 0.5 mA h cm^{-2}.

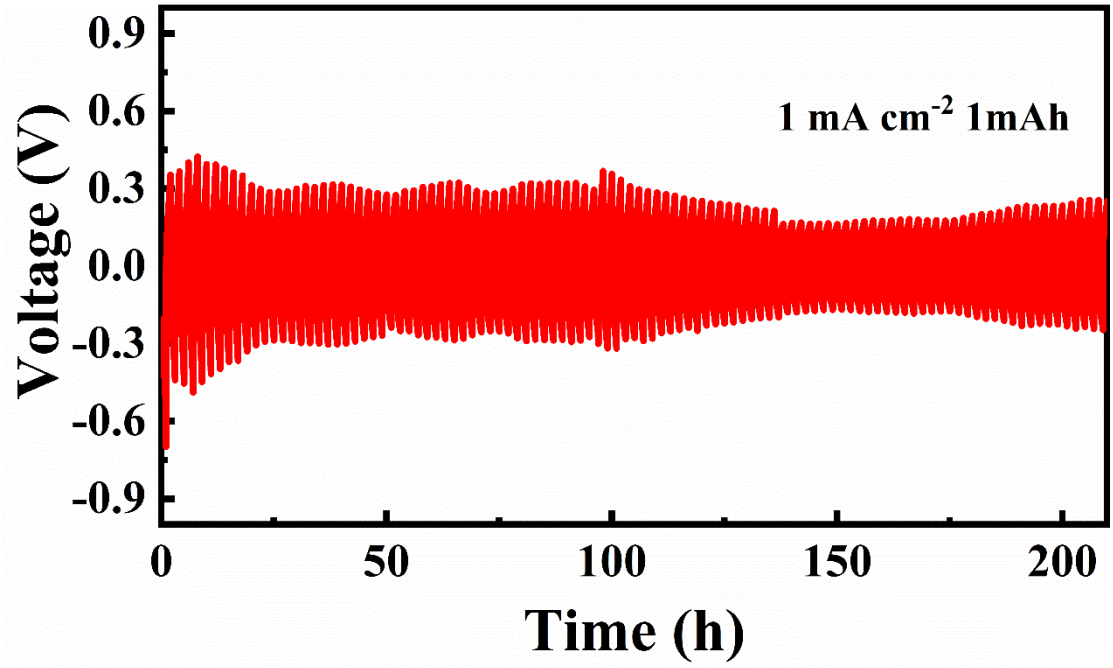

Figure S15. Galvanostatic Zn plating/stripping in Zn//Zn symmetrical cells with ZLU electrolyte at 1 mA cm^{-2} and 1 mA h cm^{-2}.

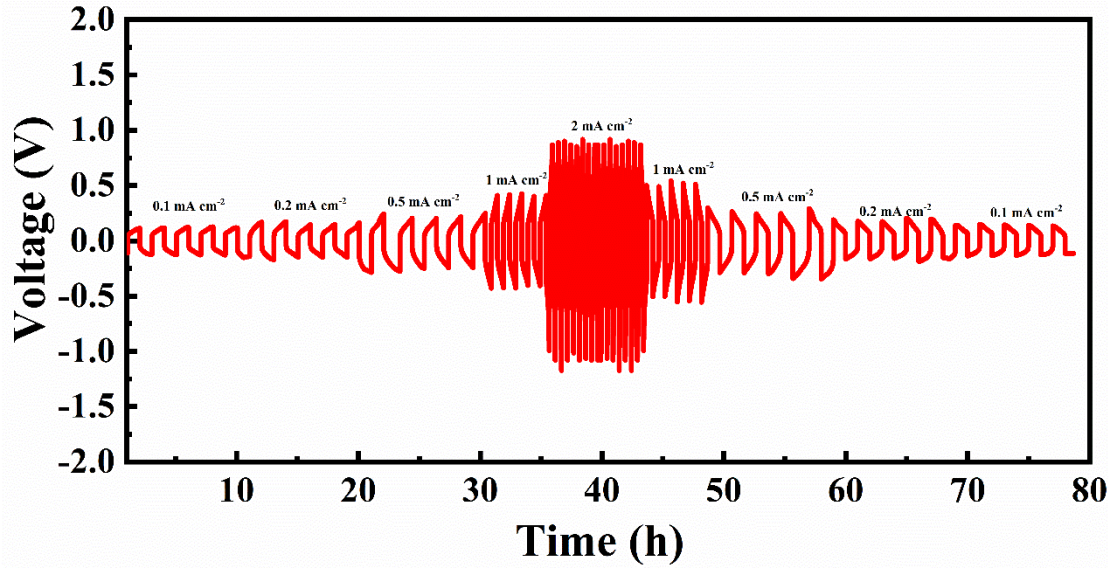

Figure S16. Galvanostatic Zn plating/stripping in Zn//Zn symmetrical cells with ZLU electrolyte at different current densities.

The DOD is respectively 0.86%, 1.71%, 4.3% and 8.5% (0.1 mAh/cm^{-2}, 0.2 mAh cm^{-2}, 0.5 mAh cm^{-2} and 1 mAh cm^{-2}).

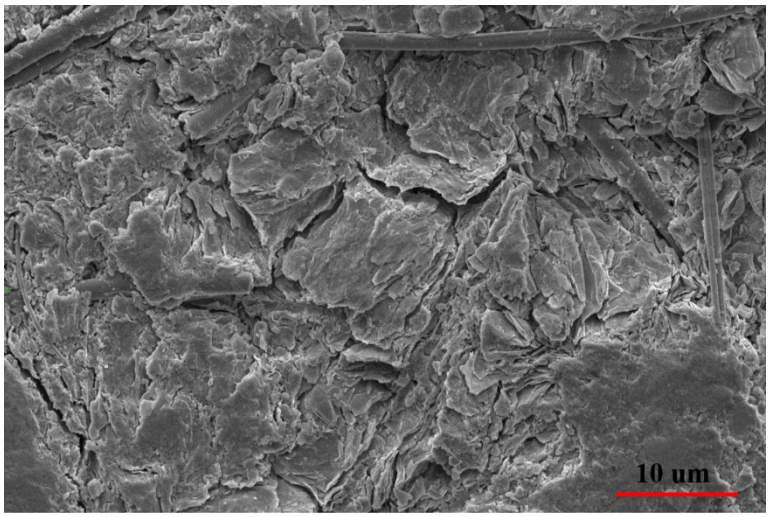

Figure S17. SEM images of cycled Zn in Zn//Zn symmetrical cells using AQ electrolyte.

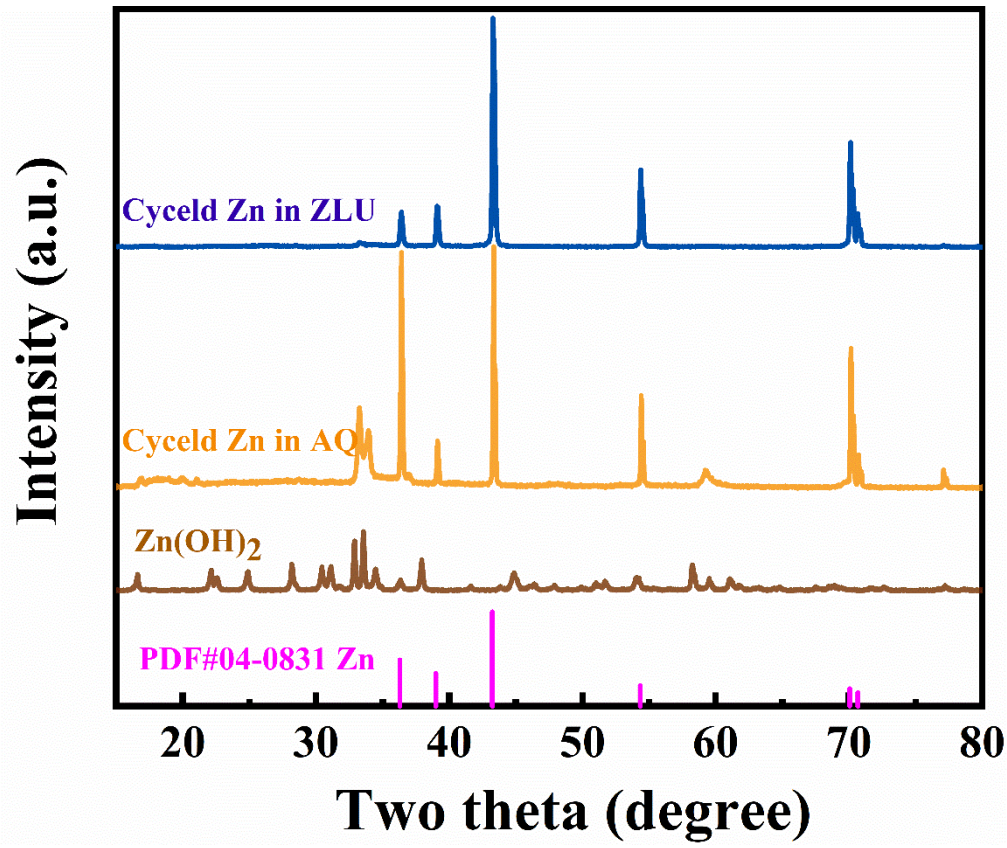

Figure S18. XRD profiles of the cycled Zn with AQ and ZLU electrolyte.

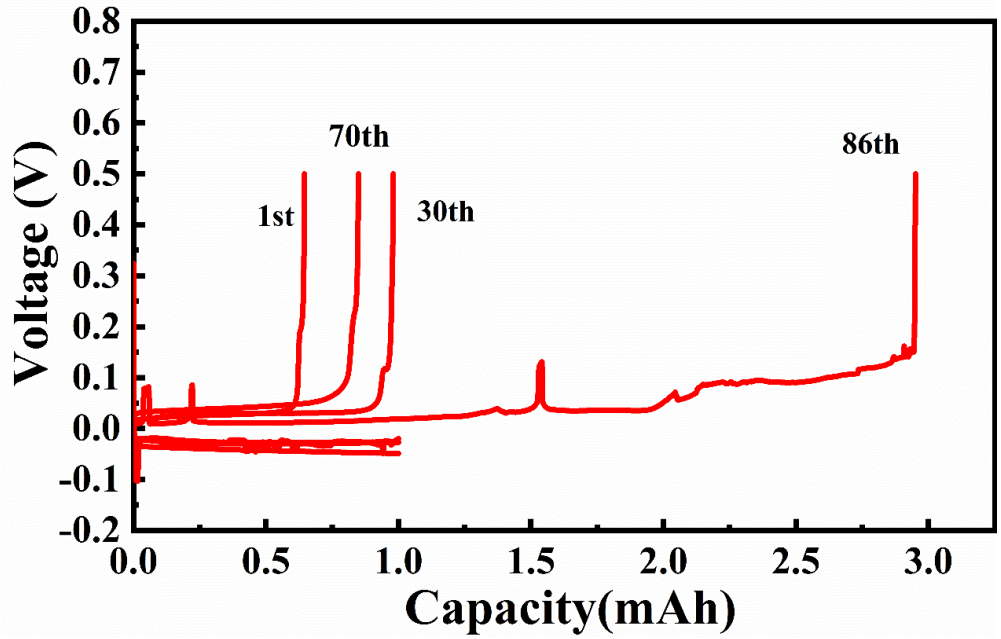

Figure S19. Zn plating/stripping voltage profiles of Zn//Cu asymmetrical cells using reference AQ electrolyte.

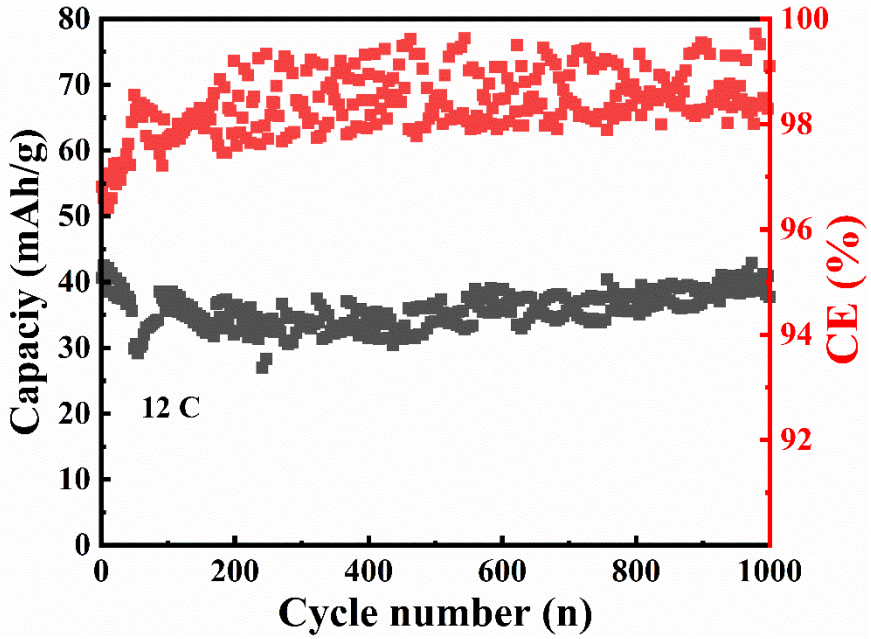

Figure S20. Cycling stability and coulombic efficiency of full battery with free-anode (Cu current collector was used as negative electrode) employing ZLU eutectic electrolyte at 12 C.

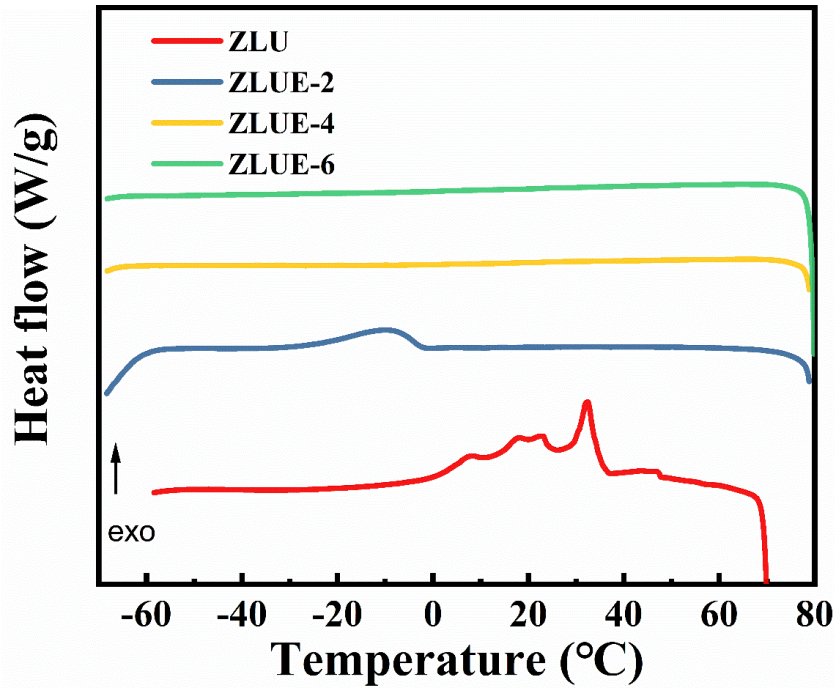

Figure S21. DSC profiles of ZLU, ZLUE-2, ZLUE-4 and ZLUE-6 eutectic electrolyte from -70 to 80 °C.

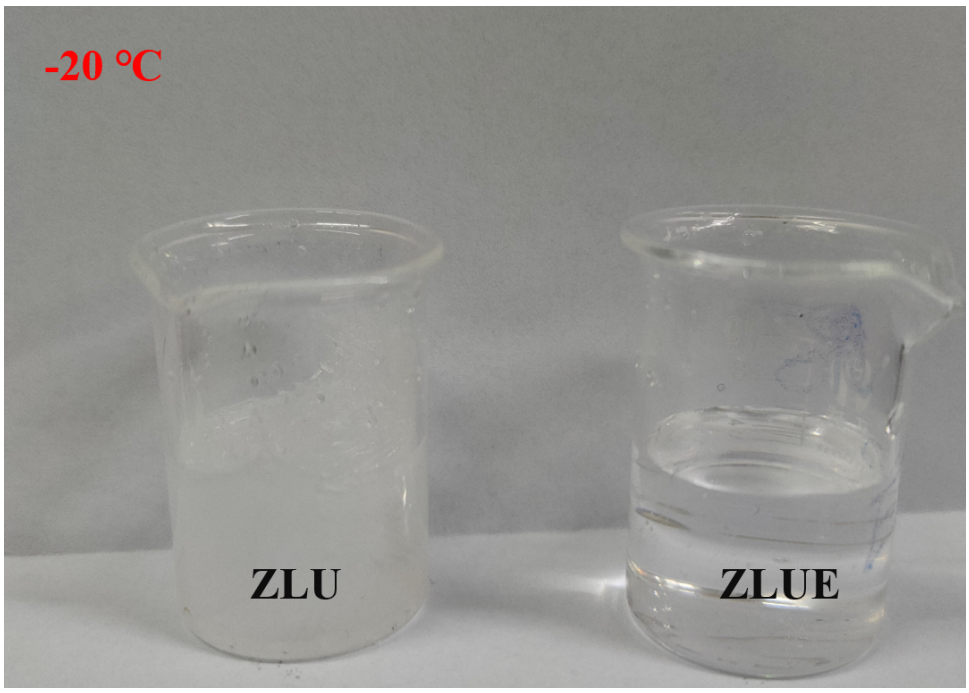

Figure S22. Optical photos of ZLU and ZLUE eutectic electrolyte at -20 °C.

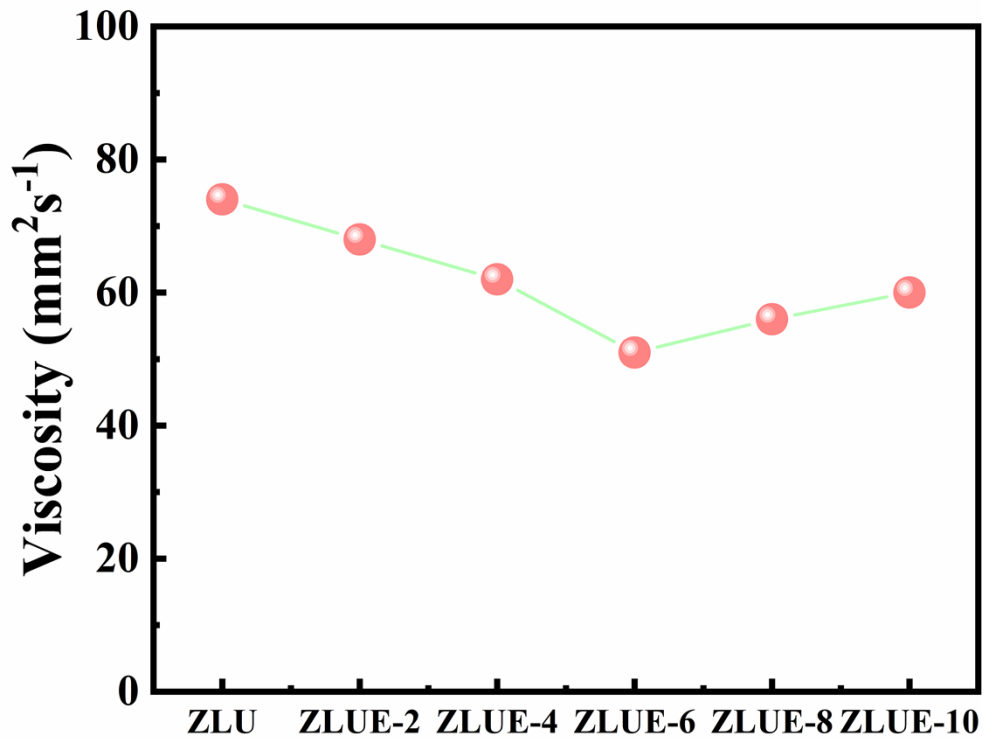

Figure S23. Viscosity of ZLU and ZLUE eutectic electrolyte with different contents of EG at 25°C.

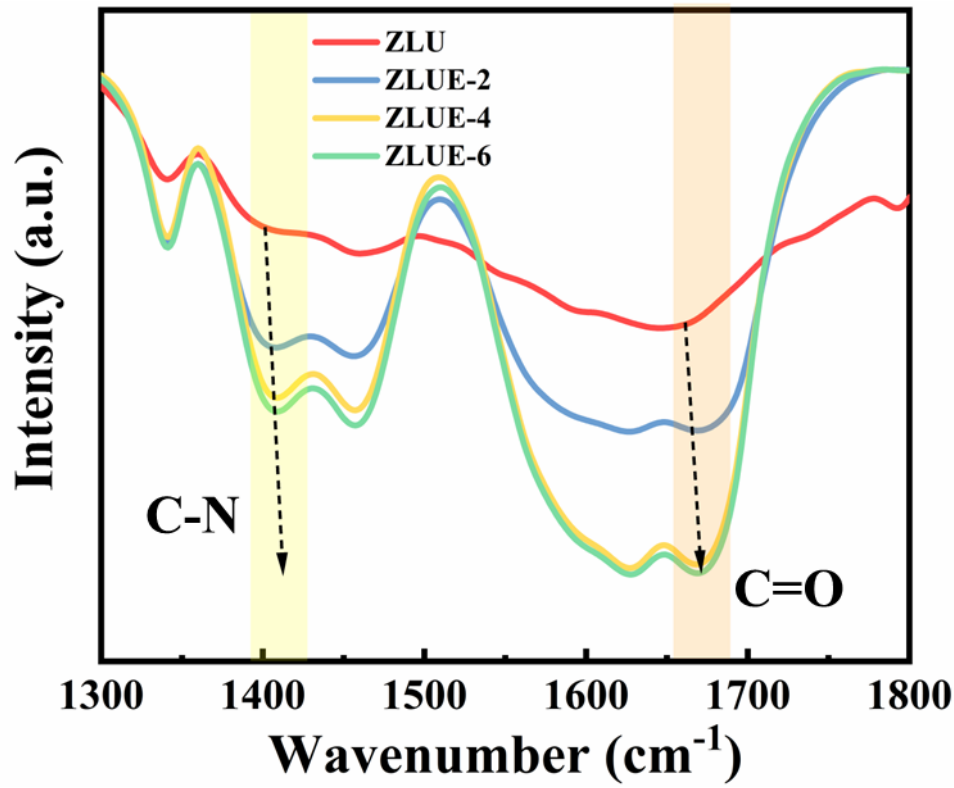

Figure S24. FTIR spectra of the C–N and C=O stretching vibration with different contents of EG.

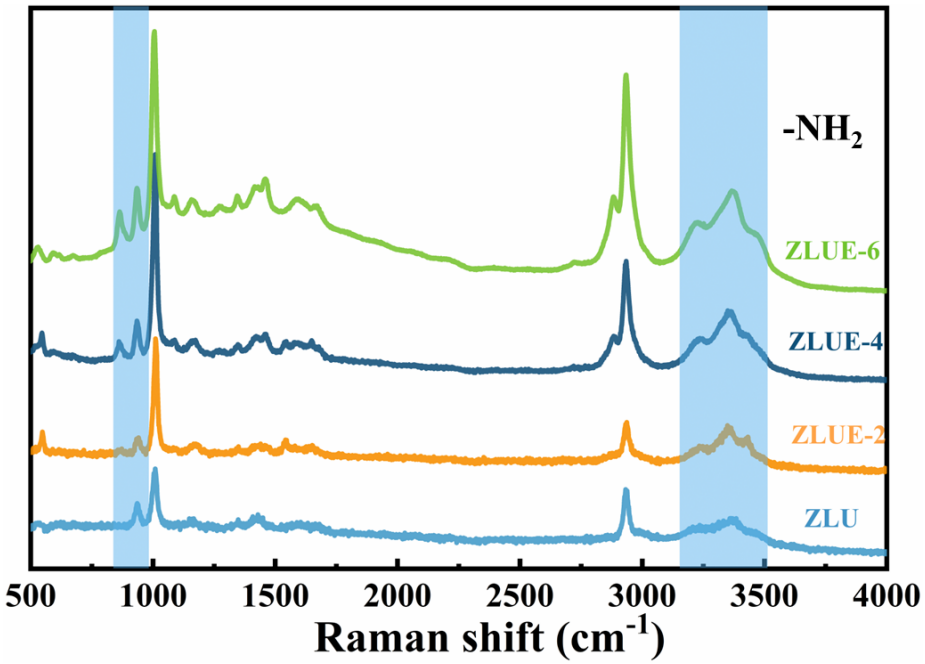

Figure S25. Raman spectra of eutectic electrolyte with different contents of EG.

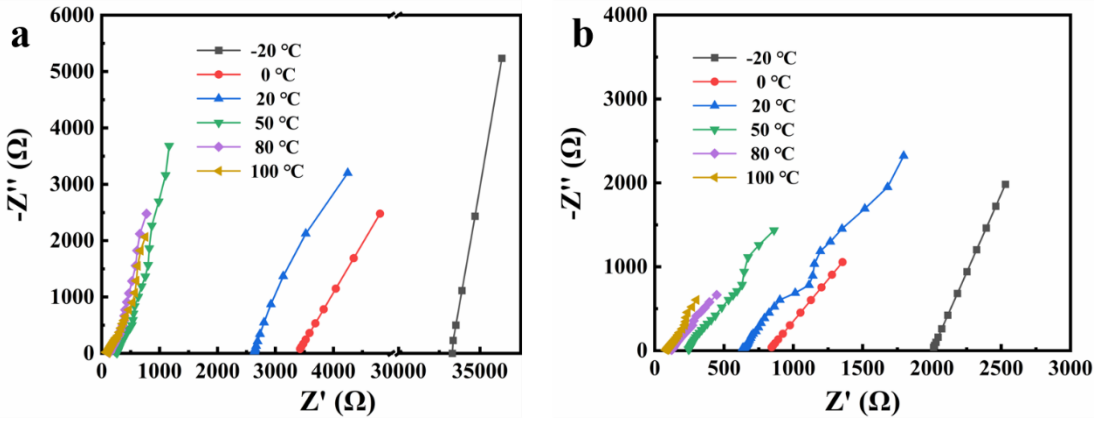

Figure S26. EIS of ZLU (a) and ZLUE (b) at vary temperature.

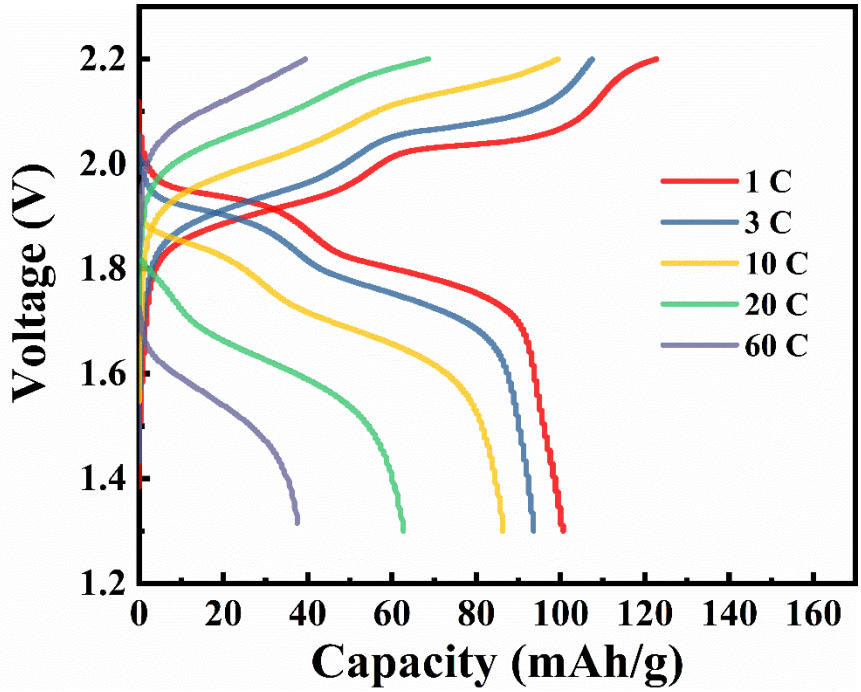

Figure S27. The rate capability (Zn//LMO full battery) in ZLUE eutectic electrolyte.

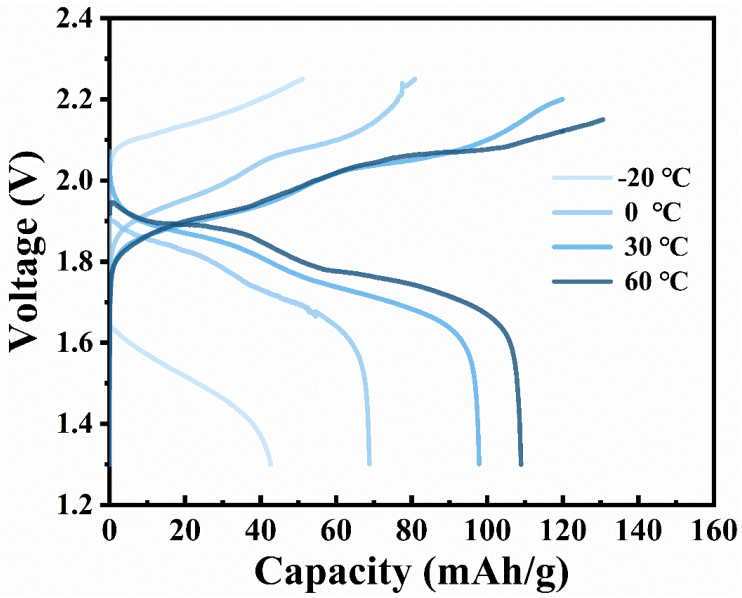

Figure S28. The capacity of Zn//LMO full battery employing ZLUE eutectic electrolyte over a wide range temperature at 2 C.

Table S2. Comparison of cycle stability between our developed Zn//LMO full battery employing ZLUE eutectic electrolyte and reported representative other batteries.

Cathode	***Anode***	***Electrolyte***	***Capacity retention (cycles)***	***Ref.***
$LiMn_2O_4$	VO_2	Saturated $LiNO_3$	83% (42)	[7]
$LiMn_2O_4$	V_2O_5	Saturated $LiNO_3$	89% (100)	[8]
$LiMn_2O_4$	$LiTi_2(PO_4)_3$	1 M Li_2SO_4	82% (200)	[9]
$LiMn_2O_4$/CNT	Li foil	1M $LiPF_6$ (EC/DMC/EMC)	92% (50)	[10]
Porous $LiMn_2O_4$	Metallic lithium	1 M $LiPF_6$ (EC/DMC)	73% (1000)	[11]
$LiMn_2O_4$	Zn foil	Thixotropic gel	61% (1000)	[12]
$LiMn_2O_4$	Zn foil	Pb^{2+}-containing gel	75% (300)	[13]
$LiMn_2O_4$ with RGO films	Zn foil	1 M Li_2SO_4+2 M $ZnSO_4$	87% (600)	[14]
$LiMn_2O_4$	Zn foil	1 M $Zn(OTf)_2$+20 M LiTFSI	92% (300)	[15]
$LiMn_2O_4$	Zn foil	ZLUE eutectic electrolyte	92% (920)	This work

Table S3. Comparison of cycle stability between our developed Zn//LMO full battery employing ZLUE eutectic electrolyte and reported representative other batteries.

Batter Type	Cathode	Anode	Energy density Wh/kg (Power density W/kg)	Ref.
Li-ion battery	**$LiMn_2O_4$**	**VO_2**	**75 (8)**	**16**
	$LiMn_2O_4$	$LiTi_2(PO_4)_3$	60 (240)	9
	$LiMn_2O_4$	LiV_3O_8	55 (11)	17
Na-ion battery	$NaTi_2(PO_4)_3$	$Na_{0.44}MnO_2$	33 (165)	18
	$NaTi_2(PO_4)_3$	$K_{0.27}MnO_2$	55 (110)	19
	CuHCF	MnHCF	27 (27)	20
Zn-dual ion battery	ZnHCF	Zn foil	100 (100)	21
	$Na_{0.95}MnO_2$	Zn foil	78 (156)	22
	CuHCF	Zn foil	52 (477)	23
	$Na_3V_2(PO_4)_3$	Zn foil	90 (88)	24
	$LiMn_2O_4$	Zn foil	197 (295)	This work

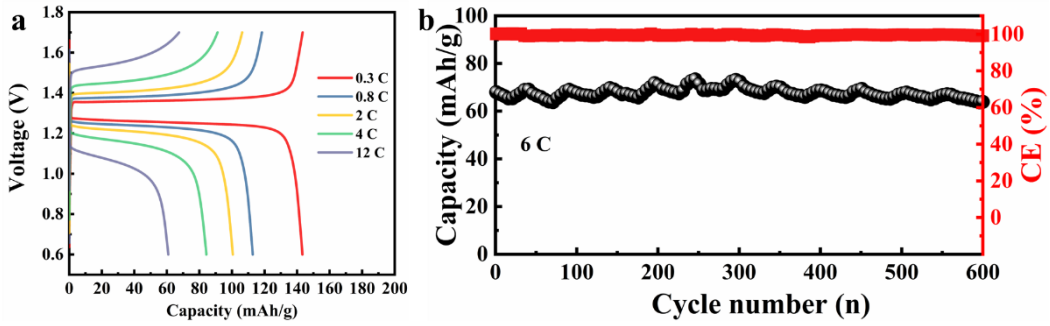

Figure S29. (a) The rate capability (Zn//LFP full battery) in ZLUE eutectic electrolyte. (b) Cycling stability and coulombic efficiency of Zn//LFP full battery at 6 C.

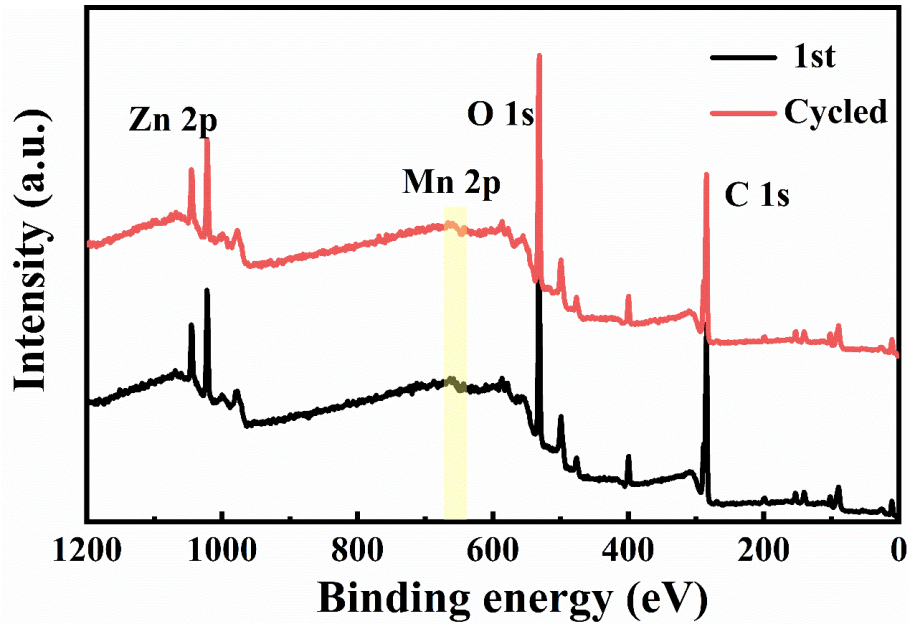

Figure S30. XPS spectra of 1st cycled LMO and cycled LMO with 200 cycles.

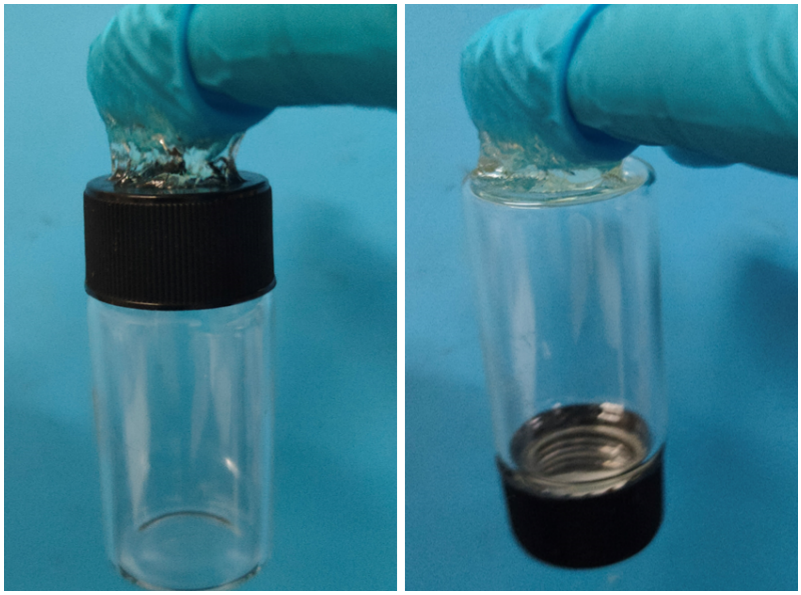

Figure S31. Adhesive photos between PZLUE eutetogel and glass bottles and glass caps.

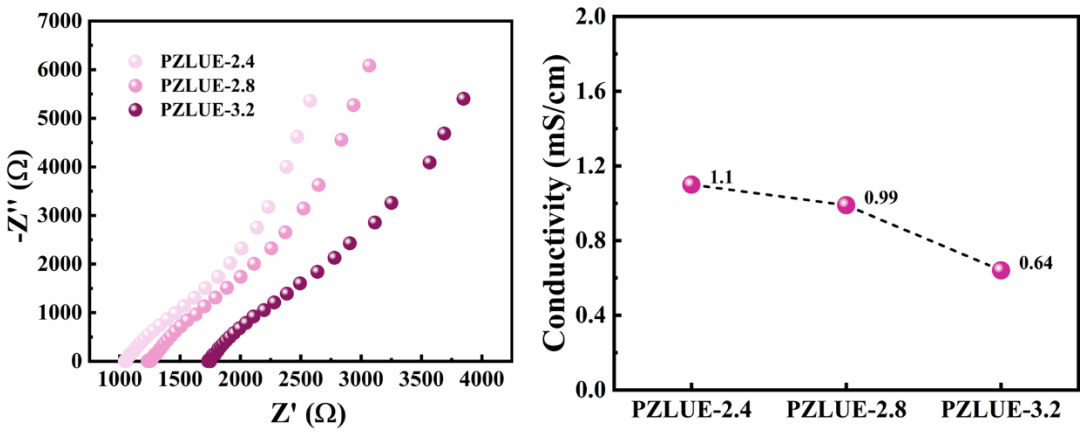

Figure S32. EIS data and ionic conductivity of PZLUE eutetogel with different contents of Aam monomer.

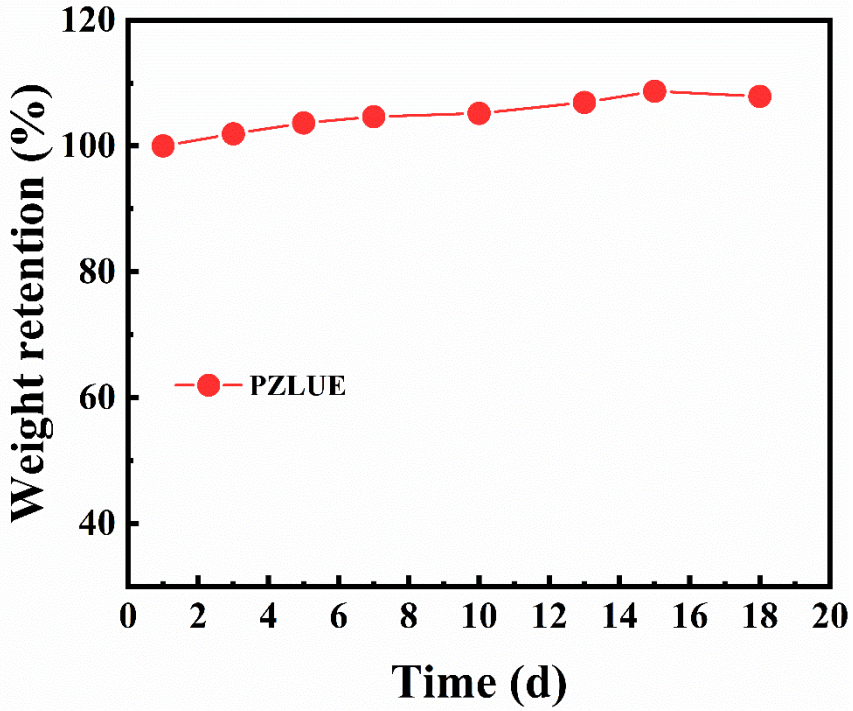

Figure S33. Volatility tests of PZLUE eutetogel in the atmosphere for 18 days at room temperature.

Table S4. Comparison of cycling life of Zn//Zn cells between our developed eutectic electrolyte and eutectogel and other reported Zn//Zn cells.

Electrolyte composition	CE (%)	Cycling life of Zn//Zn cells	Ref.
4 M $ZnSO_4$	97	250 h at 0.25 mA cm^{-2}, 0.25 mA h cm^{-2}	25
4 M $Zn(TFSI)_2$	99	770 h at 0.25 mA cm^{-2}, 0.25 mA h cm^{-2}	25
30 m $ZnCl_2$	95.4	600 h at 0.2 mA cm^{-2}, 0.2 mA h cm^{-2}	26
$ZnCl_2$ + $Zn(OAc)_2 \cdot 2H_2O$ (molar ratio 10:6)	99.59	1200 h at 0.2 mA cm^{-2}, 0.2 mA h cm^{-2}	27
18 m $NaClO_4$ + 0.5 m $Zn(ClO_4)_2$	98.2	1200 h at 0.2 mA cm^{-2}, 0.2 mA h cm^{-2}	28
30 m KAc + 3 m LiAc + 3 m $ZnAc_2$	99.6	1000 h at 0.1 mA cm^{-2}, 0.2 mA h cm^{-2}	29
SN/H_2O/$Zn(ClO_4)_2$	98.4	800 h at 0.05 mA cm^{-2}, 0.5 mA h cm^{-2}	30
DMC/H_2O/$Zn(OTf)_2$	99.8	1000 h at 1 mA cm^{-2}, 0.5 mA h cm^{-2}	31
DMSO/H_2O/$ZnCl_2$	99.5	1000 h t 0.5 mA cm^{-2}, 0.5 mA h cm^{-2}	32
ZLU eutectic electrolyte	99.7	920 h at 0.5 mA cm^{-2}, 0.5 mA h cm^{-2}	This work
PZLUE eutectogel	99.8	1130 h at 0.5 mA cm^{-2}, 0.5 mA h cm^{-2}	This work

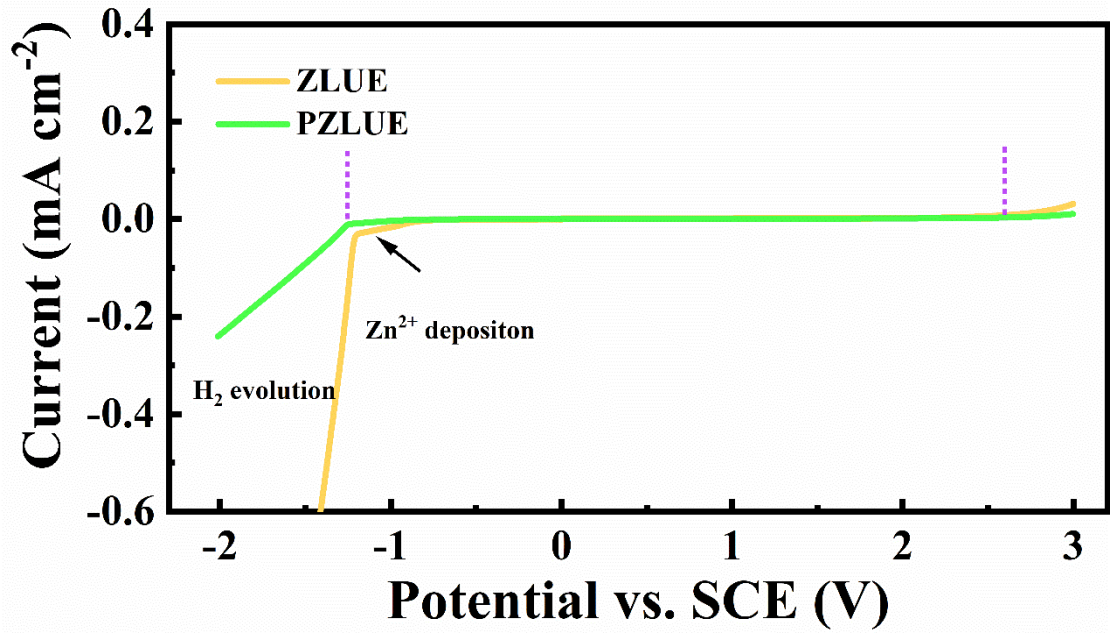

Figure S34. Electrochemical stability window of ZLUE and PZLUE eutectic electrolyte.

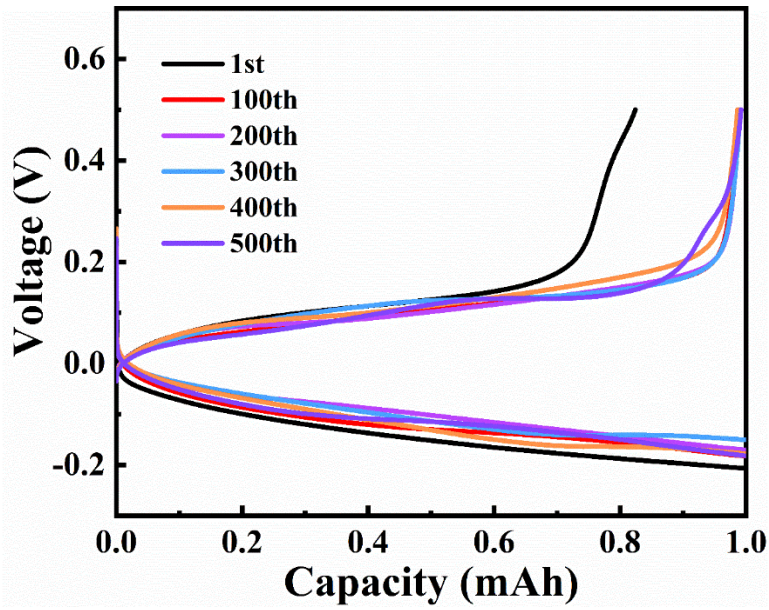

Figure S35. Zn plating/stripping voltage profiles of Zn//Cu asymmetrical cells employing PZLUE eutetogel electrolyte.

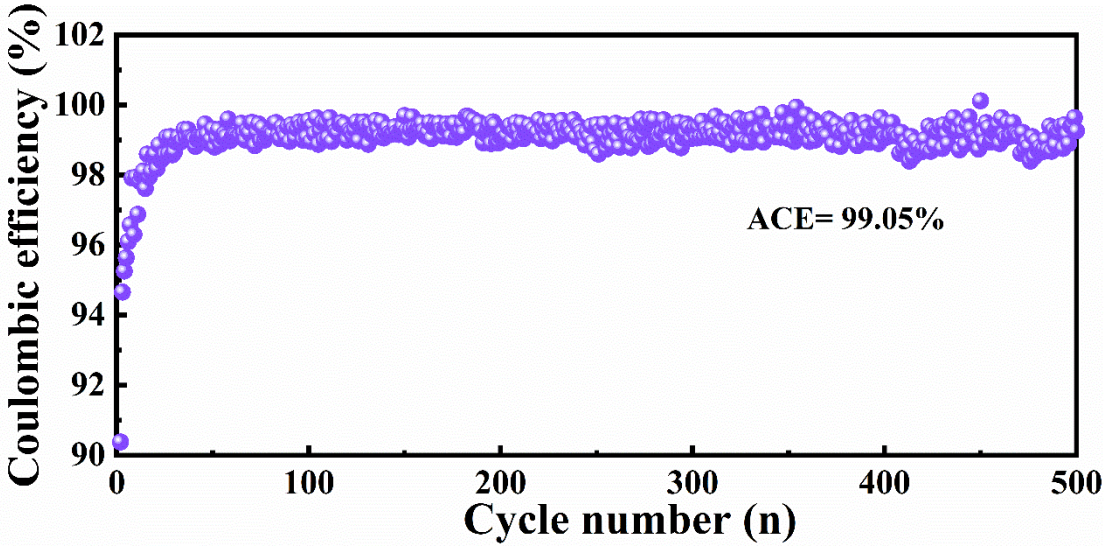

Figure S36. CE of Zn//Cu asymmetrical cells employing PZLUE eutectogel electrolyte.

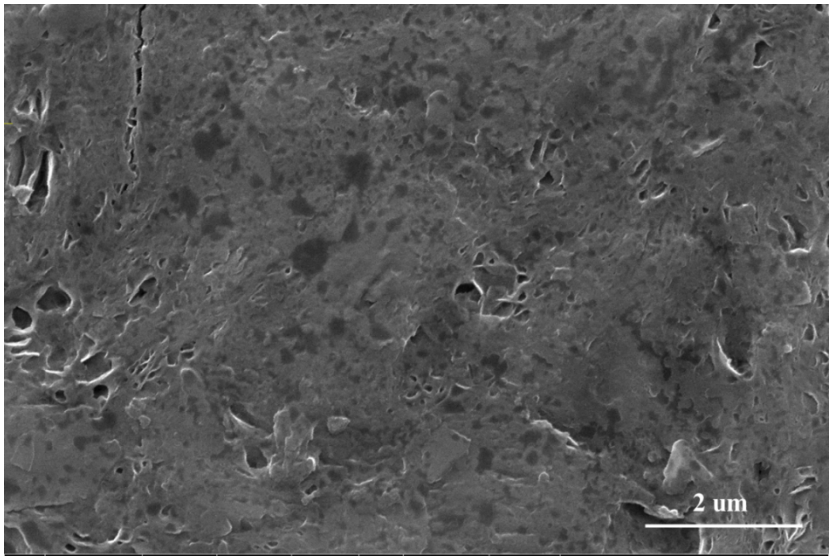

Figure S37. SEM image of the cycled Zn anode in the Zn//Zn cells with PZLUE eutetogel.

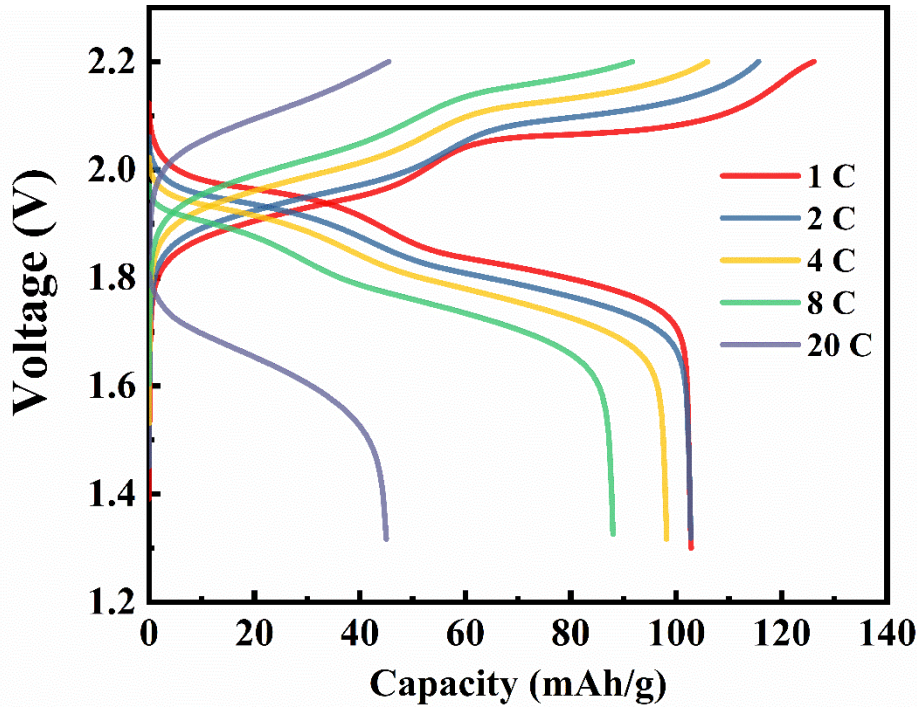

Figure S38. The rate capability (Zn//LMO) in PZLUE eutetogel electrolyte.

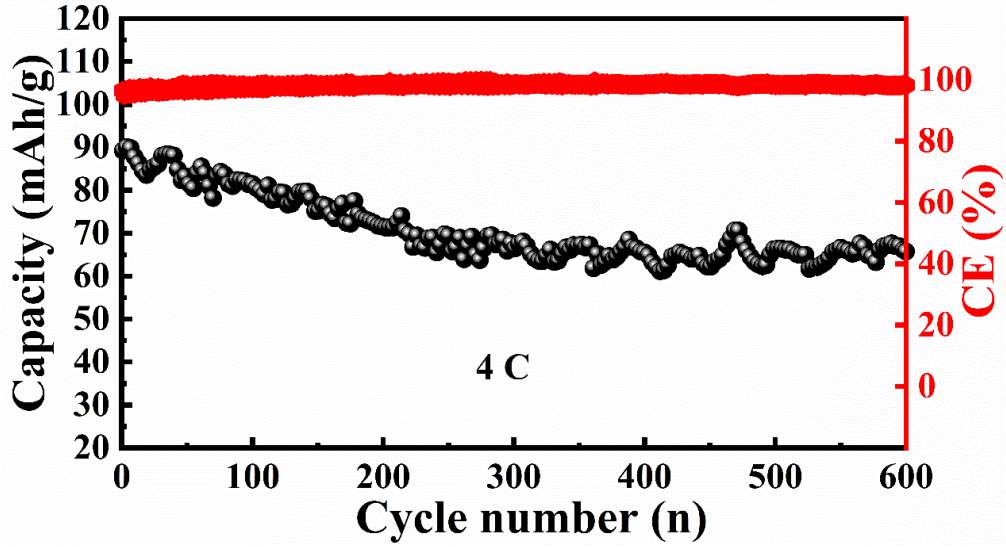

Figure S39. Cycling stability and coulombic efficiency of Zn//LMO full battery employing PZLUE eutetogel electrolyte at 4 C.

Reference

1. L. Suo, O. Borodin, T. Gao, M. Olguin, J. Ho, X. Fan, C. Luo, C. Wang and K. Xu, *Science*,

2015, **350**, 938-943.
2. L. Suo, O. Borodin, W. Sun, X. Fan, C. Yang, F. Wang, T. Gao, Z. Ma, M. Schroeder, A. von Cresce, S. M. Russell, M. Armand, A. Angell, K. Xu and C. Wang, *Angew Chem Int Ed Engl*, 2016, **55**, 7136-7141.
3. Y. Yamada, K. Usui, K. Sodeyama, S. Ko, Y. Tateyama and A. Yamada, *Nature Energy*, 2016, **1**.
4. F. Wang, O. Borodin, M. S. Ding, M. Gobet, J. Vatamanu, X. Fan, T. Gao, N. Eidson, Y. Liang, W. Sun, S. Greenbaum, K. Xu and C. Wang, *Joule*, 2018, **2**, 927-937.
5. S. Ko, Y. Yamada, K. Miyazaki, T. Shimada, E. Watanabe, Y. Tateyama, T. Kamiya, T. Honda, J. Akikusa and A. Yamada, *Electrochemistry Communications*, 2019, **104**.
6. J. Forero-Saboya, E. Hosseini-Bab-Anari, M. E. Abdelhamid, K. Moth-Poulsen and P. Johansson, *J Phys Chem Lett*, 2019, **10**, 4942-4946.
7. H. Wang, K. Huang, Y. Zeng, S. Yang and L. Chen, *Electrochimica Acta*, 2007, **52**, 3280-3285.
8. I. Stojković, N. Cvjetićanin, I. Pašti, M. Mitrić and S. Mentus, *Electrochemistry Communications*, 2009, **11**, 1512-1514.
9. J. Y. Luo and Y. Y. Xia, *Advanced Functional Materials*, 2007, **17**, 3877-3884.
10. M. Tang, A. Yuan and J. Xu, *Electrochimica Acta*, 2015, **166**, 244-252.
11. L. J. Xi, H.-E. Wang, Z. G. Lu, S. L. Yang, R. G. Ma, J. Q. Deng and C. Y. Chung, *Journal of Power Sources*, 2012, **198**, 251-257.
12. T. K. A. Hoang, T. N. L. Doan, C. Lu, M. Ghaznavi, H. Zhao and P. Chen, *ACS Sustainable Chemistry & Engineering*, 2016, **5**, 1804-1811.
13. T. K. A. Hoang, M. Acton, H. T. H. Chen, Y. Huang, T. N. L. Doan and P. Chen, *Materials Today Energy*, 2017, **4**, 34-40.
14. J. Zhi, A. Z. Yazdi, G. Valappil, J. Haime and P. Chen, 2017, **3**, e1701010.
15. A. Clarisza, H. K. Bezabh, S. K. Jiang, C. J. Huang, B. W. Olbasa, S. H. Wu, W. N. Su and B. J. Hwang, *ACS Appl Mater Interfaces*, 2022, **14**, 36644-36655.
16. W. Li, J. R. Dahn and D. S. Wainwright, 1994, **264**, 1115-1118.
17. G. J. Wang, H. P. Zhang, L. J. Fu, B. Wang and Y. P. Wu, *Electrochemistry Communications*, 2007, **9**, 1873-1876.
18. Z. Li, D. Young, K. Xiang, W. C. Carter and Y.-M. Chiang, *Advanced Energy Materials*, 2013, **3**, 290-294.
19. Y. Liu, Y. Qiao, W. Zhang, H. Xu, Z. Li, Y. Shen, L. Yuan, X. Hu, X. Dai and Y. Huang, *Nano Energy*, 2014, **5**, 97-104.
20. M. Pasta, C. D. Wessells, N. Liu, J. Nelson, M. T. McDowell, R. A. Huggins, M. F. Toney and Y. Cui, *Nat Commun*, 2014, **5**, 3007.
21. L. Zhang, L. Chen, X. Zhou and Z. Liu, *Advanced Energy Materials*, 2015, **5**.
22. B. Zhang, Y. Liu, X. Wu, Y. Yang, Z. Chang, Z. Wen and Y. Wu, *Chem Commun (Camb)*, 2014, **50**, 1209-1211.
23. R. Trocoli and F. La Mantia, *ChemSusChem*, 2015, **8**, 481-485.
24. G. Li, Z. Yang, Y. Jiang, C. Jin, W. Huang, X. Ding and Y. Huang, *Nano Energy*, 2016, **25**, 211-217.
25. N. Patil, C. Cruz, D. Ciurduc, A. Mavrandonakis, J. Palma and R. Marcilla, *Adv. Energy Mater.*, 2021, **11**, 2100939.
26. C. Zhang, J. Holoubek, X. Wu, A. Daniyar, L. Zhu, C. Chen, D. P. Leonard, I. A. Rodríguez-

Pérez, J.-X. Jiang, C. Fang and X. Ji, *Chemical Communications*, 2018, **54**, 14097-14099.
27. M. Yang, J. Zhu, S. Bi, R. Wang and Z. Niu, *Adv Mater*, 2022, **34**, e2201744.
28. Y. Zhu, J. Yin, X. Zheng, A.-H. Emwas, Y. Lei, O. F. Mohammed, Y. Cui and H. N. Alshareef, *Energy & Environmental Science*, 2021, **14**, 4463-4473.
29. J. Han, A. Mariani, A. Varzi and S. Passerini, *Journal of Power Sources*, 2021, **485**, 229329.
30. W. Yang, X. Du, J. Zhao, Z. Chen, J. Li, J. Xie, Y. Zhang, Z. Cui, Q. Kong, Z. Zhao, C. Wang, Q. Zhang and G. Cui, *Joule*, 2020, **4**, 1557-1574.
31. Y. Dong, L. Miao, G. Ma, S. Di, Y. Wang, L. Wang, J. Xu and N. Zhang, *Chemical Science*, 2021, **12**, 5843-5852.
32. L. Cao, D. Li, E. Hu, J. Xu, T. Deng, L. Ma, Y. Wang, X.-Q. Yang and C. Wang, *Journal of the American Chemical Society*, 2020, **142**, 21404-21409.